FULL PAPER

Dalton
www.rsc.org/dalton

From model compounds to protein binding: syntheses, characterizations and fluorescence studies of $[Ru^{II}(bipy)(terpy)L]^{2+}$ complexes (bipy = 2,2′-bipyridine; terpy = 2,2′:6′,2″-terpyridine; L = imidazole, pyrazole and derivatives, cytochrome *c*)†

Xiao-Juan Yang,[a] Friedrich Drepper,[b] Biao Wu,[a] Wen-Hua Sun,[c] Wolfgang Haehnel[b] and Christoph Janiak*[a]

[a] *Institut für Anorganische und Analytische Chemie, Universität Freiburg, Albertstr. 21, 79104, Freiburg, Germany. E-mail: janiak@uni-freiburg.de; Fax: 49 761 2036147; Tel: 49 761 2036127*

[b] *Institut für Biologie 2, Universität Freiburg, Schänzlestraße 1, 79104, Freiburg, Germany*

[c] *CAS Key Laboratory of Engineering Plastics, Institute of Chemistry, Chinese Academy of Sciences, Beijing, 100080, People's Republic of China*

Received 28th September 2004, Accepted 19th November 2004
First published as an Advance Article on the web 9th December 2004

Compounds $[Ru^{II}(bipy)(terpy)L](PF_6)_2$ with bipy = 2,2′-bipyridine, terpy = 2,2′:6′,2″-terpyridine, L = H_2O, imidazole (imi), 4-methylimidazole, 2-methylimidazole, benzimidazole, 4,5-diphenylimidazole, indazole, pyrazole, 3-methylpyrazole have been synthesized and characterized by ^{1}H NMR, ESI-MS and UV/Vis (in CH_3CN and H_2O). For L = H_2O, imidazole, 4,5-diphenylimidazole and indazole the X-ray structures of the complexes have been determined with the crystal packing featuring only few intermolecular C–H $\cdots$ π or π–π interactions due to the separating action of the PF_6-anions. Complexes with L = imidazole and 4-methylimidazole exhibit a fluorescence emission with a maximum at 662 and 667 nm, respectively (λ_{exc} = 475 nm, solvent CH_3CN or H_2O). The substitution of the aqua ligand in $[Ru(bipy)(terpy)(H_2O)]^{2+}$ in aqueous solution by imidazole to give $[Ru(bipy)(terpy)(imi)]^{2+}$ is fastest at a pH of 8.5 (as followed by the increase in emission intensity). Coupling of the $[Ru(bipy)(terpy)]^{2+}$ fragment to cytochrome *c* (Yeast iso-1) starting from the Ru-aqua complex was successful at 35 °C and pH 7.0 after 5 d under argon in the dark. The [Ru(bipy)(terpy)(cyt *c*)]-product was characterized by UV/Vis, emission and mass spectrometry. The location where the [Ru(bipy)(terpy)] complex was coupled to the protein was identified as His44 (corresponding to His39 in other numbering schemes) using digestion of the Ru-coupled protein by trypsin and analysis of the tryptic peptides by HPLC-high resolution MS.

Introduction

Complexes of ruthenium(II) with polypyridyl ligands have been of great interest for decades in a variety of areas such as photophysics, photochemistry and photoredox chemistry, because of their interesting excited-state properties.[1–3] One of the important recent applications of ruthenium polypyridyl compounds is the study of photo-induced energy and electron transfer processes.[4] For instance, the $[Ru(bipy)_2(bipy')]^{2+}$ and $[Ru(bipy)_2L_2]^{2+}$ complexes (bipy = 2,2′-bipyridine; bipy′ = substituted 2,2′-bipyridine) have been used in the binding of proteins and for the energy or electron transfer within the modified proteins.[5] The $[Ru(bipy)_2(bipy')]^{2+}$ complexes, where bipy′ denotes 2,2′-bipyridine derivatives with functional groups such as $-CH_2Br$, have been coupled to cysteine or lysine residues of proteins through the functional groups of bipy′.[6–8] In the case of $[Ru(bipy)_2(H_2O)L]^{2+}$ (L = H_2O or imidazole) the binding of proteins occurs through the coordination of the ruthenium(II) ion by the imidazole nitrogen atom of the histidine residue in proteins such as cytochrome *c* (cyt *c*) and others.[9,10]

The ruthenium-coupled proteins such as $[cis\text{-}Ru(bipy)_2(imi)(protein)]^{2+}$ systems (imi = imidazole) are of particular interest in the electron transfer reactions due to their long-lived excited states.[9,10] Various electron transfer processes have been studied in $[Ru(bipy)_2(imi)(His33\text{-}cyt\ c)]^{2+}$.[9] However, there are two free sites in the starting material $[Ru(CO_3)(bipy)_2]$ or $[Ru(bipy)_2(H_2O)_2]^{2+}$ which can be bonded by imidazole and the coupling is accomplished by two steps: first binding of the protein to $[Ru(bipy)_2(H_2O)_2]^{2+}$ to form $[Ru(bipy)_2(H_2O)(protein)]^{2+}$; then substitution of the second H_2O molecule by imidazole to form $[Ru(bipy)_2(imi)(protein)]^{2+}$ (eqn. (1)).

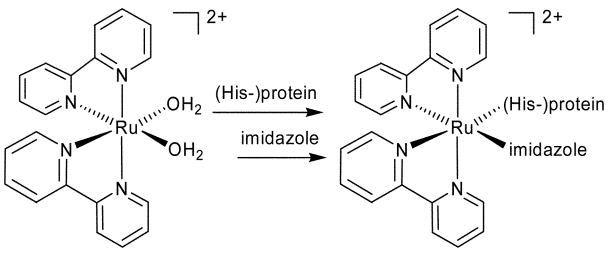

(1)

This sequence may lead to competition reactions during the substitution of the water molecule by imidazole and the protein. In an attempt to avoid such difficulties, we chose the terpy analogues $[Ru(bipy)(terpy)Cl]^+$ or $[Ru(bipy)(terpy)(H_2O)]^{2+}$ (terpy = 2,2′:6′,2″-terpyridine) as precursors for protein coupling. These mixed terpy–bipy complexes have only one coordination site remaining to be occupied by the protein and the protein coupling can be simplified to a one-step reaction (eqn. (2)).

† Electronic supplementary information (ESI) available: Listing and discussion of π–π and C–H $\cdots$ π stacking in the crystal structure of compounds **1**, **5**·CH_3OH, **6** and Ru–H_2O. See http://www.rsc.org/suppdata/dt/b4/b414999h/

DOI: 10.1039/b414999h

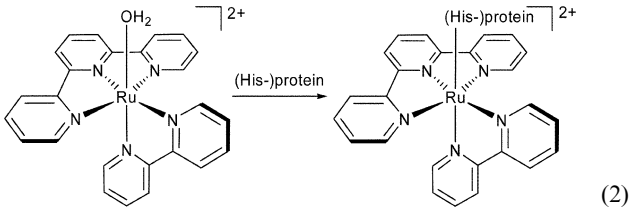

(2)

Previously we have bound $Ru(bipy)_2$(4-methyl-4′-bromomethyl-bipy) to cysteine.[8] The resulting linker $–CH_2–S–CH_2–$ to the protein backbone provides considerable flexibility which makes a prediction of the electron transfer pathway difficult. In addition Cys inserted at the protein surface may lead to a dimerization. Therefore coupling of $[Ru^{II}(bipy)(terpy)]^{2+}$ to a His has considerable advantages including the very short linkage *via* the $–CH_2–$ of His. Complexes of the tridentate terpy ligand have attracted much attention recently[11] and the syntheses and properties of $[Ru(bipy)(terpy)L]^{n+}$ complexes, where L is a monodentate ligand such as H,[12] H_2O,[13] NH_3,[14] pyridine (py),[15–17] pyrazine (pz)[18] *etc.* have been studied. Structures for $[Ru(bipy)(terpy)L]^{n+}$ are known with the nitrogen donor ligands L = isopropylideneamido,[19] 2,4-dichlorophenyl-, 4-iodophenyl- and μ-4,4′-azodi(phenylcyanamido),[20–22] μ-1,4-bis(2-(4-(cyanamido)phenyl)ethynyl)benzene,[23] pyrazine,[18] pyridine,[16] 4-(acetylene)- and 4-(phenylacetylene)pyridine,[15] μ-4,4′-biypridine,[24] 2,2′-bipyridine[25] and acetonitrile.[15] Structures for $[Ru(bipy)(terpy)L]^{2+}$ complexes with L = imidazole, pyrazole or derivatives appear to be unknown.[26]

We report here the syntheses, structures, spectroscopic and fluorescence studies of $[Ru(bipy)(terpy)L](PF_6)_2$ complexes where L is imidazole, pyrazole or their derivatives and cytochrome *c* (Scheme 1).

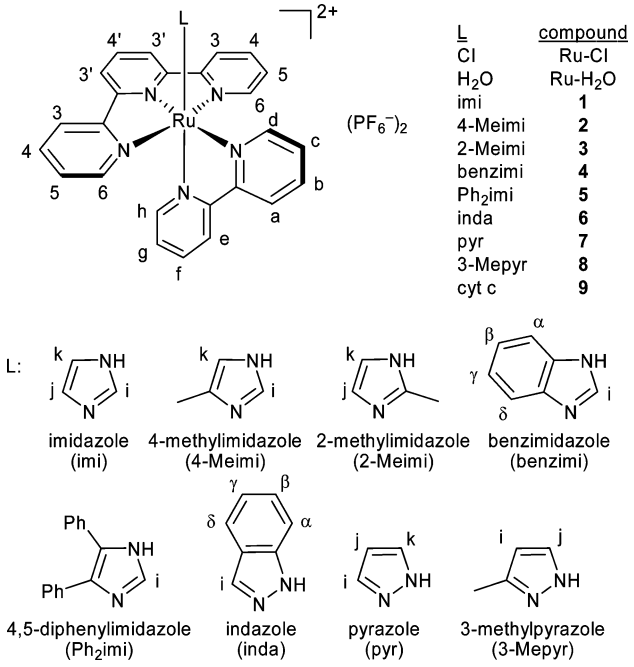

L	compound
Cl	Ru-Cl
H_2O	Ru-H_2O
imi	**1**
4-Meimi	**2**
2-Meimi	**3**
benzimi	**4**
Ph_2imi	**5**
inda	**6**
pyr	**7**
3-Mepyr	**8**
cyt c	**9**

Scheme 1 Synthesized complexes and NMR numbering scheme for $[Ru(bipy)(terpy)Cl](PF_6)$ and compounds $[Ru(bipy)(terpy)L](PF_6)_2$ (**1–8**). The complex Ru–Cl is only singly charged.

The reported studies should provide the basis for an introduction of Ru^{II}(bipy)(terpy) at a His of plastocyanin inserted by genetic engineering at a position which does not interfere with its docking sites needed for the electron transfer. The binding sites of plastocyanin have been studied in detail with photosystem I[27–29] and also with the cytochrome b_6f-complex.[30] Only two neighboring patches at the surface are involved in the docking.[30] Laser-excitation of photosystem I allows to resolve the fast 10 μs intracomplex electron transfer from plastocyanin to the reaction center of photosystem I.[28] However, the electron transfer between plastocyanin and cytochrome *f* in the cytochrome b_6f-complex was studied by stopped-flow kinetics limiting the time resolution to the mixing time of 1 ms. With the [Ru(bipy)(terpy)]-complex bound to plastocyanin we expect to be able to resolve also the intracomplex electron transfer to cytochrome *f* after excitation of the ruthenium complex with a time resolution in the range of μs and to understand the protein interaction in this important process in more detail.

Experimental

$RuCl_3 \cdot xH_2O$, 2,2′:6′,2″-terpyridine (terpy), 2,2′-bipyridine (bipy), imidazole (imi), 4-methylimidazole (4-Meimi), 2-methylimidazole (2-Meimi), benzimidazole (benzimi), 4,5-diphenylimidazole (Ph_2imi), indazole (inda), pyrazole (pyr), 3-methylpyrazole (3-Mepyr) and NH_4PF_6 were purchased from Acros or Aldrich and used as received. Other reagents and solvents were of reagent grade or better and used without further purification. Ru(terpy)Cl_3[31] and [Ru(bipy)(terpy)Cl]-PF_6[32] were prepared according to literature methods.[19,33] $[Ru(bipy)(terpy)(H_2O)](PF_6)_2$ was synthesized as in ref. 13 and single crystals for X-ray determination were obtained by recrystallization of the brown powder from hot water.

^{1}H NMR spectra were recorded on a Bruker Avance DPX200 or a Varian O-300 spectrometer (200.1 or 300.1 MHz, respectively) with calibration against the solvent signal (d_6-DMSO 2.50 ppm). UV-Vis (absorption) spectra were measured with a Shimadzu UV-2101 PC Scanning Spectrophotometer. Elemental analyses were done on a VarioEL from Elementaranalysensysteme GmbH.

Electron spray ionization mass spectra (ESI-MS) for the small molecule complexes were carried out using a Finnigan MAT LCQ Advantage. MeOH was used as the solvent. Mass spectra were measured in positive mode and in the range of m/z = 200–1400. Ruthenium containing ions had a clearly visible metal isotope pattern arising from the distribution: ^{96}Ru 17.5, ^{98}Ru 5.9, ^{99}Ru 40.2, ^{100}Ru 39.9, ^{101}Ru 53.8, ^{102}Ru 100, ^{104}Ru 59.2%.[34] Peaks were given for the most abundant ^{102}Ru isotope. The ESI-MS spectra did occasionally show traces of the $[Ru(bipy)(terpy)Cl]^+$ starting material at m/z = 526 with a maximum abundance of 5%. For the spectroscopic studies more purified samples have been used.

High-resolution mass spectra of the Ru-coupled protein and tryptic peptides were taken in ESI-positive mode on a Thermo Finnigan LTQ-FT equipped with a 7 Tesla magnet. Deconvolution of ESI charge states and isotopic patterns has been done using the Xtract program supplied by Thermo Finnigan calculating average masses of neutral molecules. HPLC (high-performance liquid chromatography, Agilent 1100) of tryptic digests of the Ru-coupled protein on a 150 mm × 300 μm reverse phase C4 column at a flow of 3 μL min^{-1} connected online to ESI-MS was used to identify the location where the [Ru(bipy)(terpy)]-complex was coupled. MS/MS spectra of the peptide fragments were taken to confirm the identity of peptides.

Emission spectra were collected on a Jobin Yvon (Instruments S.A.) Fluoromax 2 spectrometer. For emission spectra the sample was excited at the indicated wavelength (475 nm) with a spectral bandwidth of 10 nm. Fluorescence emission was detected at an angle of 90° relative to the excitation light with a spectral bandwidth of 2 nm. Wavelength calibration of the excitation and emission monochromators was done using the spectrum of the internal Xe-lamp and a Raman spectrum, respectively. Relative fluorescence yields were calculated as the ratio of emitted *vs.* absorbed light intensity normalized to the maximum emission in one series of experiments.

Syntheses

[(2,2′-Bipyridine)(imidazole)(2,2′:6′,2″-terpyridine)ruthenium-(II)] bis(hexafluorophosphate), $[Ru(bipy)(terpy)(imi)](PF_6)_2$, (1). $[Ru(bipy)(terpy)Cl]PF_6$ (50 mg, 0.074 mmol) was refluxed with

an excess of imidazole (15 mg, 0.22 mmol) in ethanol–H_2O (12 ml/12 ml) for 5 h. The volume of the solution was reduced to half by rotary evaporation. To the resulting brown solution was added solid NH_4PF_6 to form dark brown microcrystals. The product was then purified by column chromatography on silica gel (CH_3CN–toluene = 40/60) and the second band was collected. Yield: 30 mg (48%). Black single crystals were obtained by diffusion of diethyl ether into a methanol solution of the product. $C_{28}H_{23}N_7RuP_2F_{12}$ (848.54): calc.: C 39.63, H 2.73, N 11.55; found: C 39.84, H 2.79, N 11.58%. ^{1}H NMR: (DMSO-d_6, δ ppm): 12.74 (br s, 1H, NH), 8.96 (d, 1H, J = 8.4 Hz, Ha), 8.82 (d, 2H, J = 8.0, H3′), 8.73 (t, 3H, J = 7.2, H3 + e), 8.52 (d, 1H, J = 5.6, Hd), 8.38 (td, 1H, J_1 = 8.0, J_2 = 1.2, Hb), 8.26 (t, 1H, J = 8.0, H4′), 8.12 (td, 2H, J_1 = 8.0, J_2 = 1.2, H4), 7.98–7.86 (m, 2H, Hc + f), 7.81 (d, 2H, J = 4.8, H6), 7.51 (td, 2H, J_1 = 7.2, J_2 = 1.0, H5), 7.36 (d, 1H, J = 4.6, Hh), 7.18 (t, 2H, J = 5.6, Hg + k), 7.00 (s, 1H, Hi), 6.02 (s, 1H, Hj) (see Scheme 1). ESI-MS: m/z (intensity (%), fragment) 704.4 (4, $[M - PF_6^-]^+$), 558.5 (2, $[M - H^+ - 2PF_6^-]^+$), 279.7 (100, $[M - 2PF_6^-]^{2+}$).

[(2,2′-Bipyridine)(4-methylimidazole)(2,2′:6′,2″-terpyridine)-ruthenium(II)] bis(hexafluorophosphate), [Ru(bipy)(terpy)(4-Meimi)](PF$_6$)$_2$, (2). [Ru(bipy)(terpy)Cl]PF_6 (50 mg, 0.074 mmol) was refluxed with an excess of 4-methylimidazole (57 mg, 0.7 mmol) in ethanol–H_2O (15 ml/15 ml) for 5 h. The work-up was similar to that of compound **1**. After column chromatography (CH_3CN–toluene = 40/60) the product was recrystallized from acetone–EtOH. Yield: 33 mg (52%). $C_{29}H_{25}N_7RuP_2F_{12}\cdot CH_3COCH_3$ (920.64): calc.: C 41.75, H 3.39, N 10.65; found: C 41.81, H 3.38, N 10.95%. ^{1}H NMR: (DMSO-d_6, δ ppm): 12.58 (br s, 1H, NH), 8.96 (d, 1H, J = 7.9 Hz, Ha), 8.82 (d, 2H, J = 8.1, H3′), 8.72 (t, 3H, J = 7.4, H3 + e), 8.56 (d, 1H, J = 5.3, Hd), 8.38 (td, 1H, J_1 = 7.8, J_2 = 1.2, Hb), 8.26 (t, 1H, J = 8.1, H4′), 8.12 (td, 2H, J_1 = 7.8, J_2 = 1.2, H4), 8.00–7.86 (m, 2H, Hc + f), 7.79 (d, 2H, J = 4.7, H6), 7.51 (td, 2H, J_1 = 6.1, J_2 = 1.0, H5), 7.35 (d, 1H, J = 5.6, Hh), 7.18 (t, 1H, J = 6.0, Hg), 6.86 (s, 1H, Hk), 5.73 (s, 1H, Hj), 1.98 (s, 3H, CH_3). ESI-MS: m/z (intensity (%), fragment) 717.9 (82, $[M - PF_6^-]^+$), 572.0 (57, $[M - H^+ - 2PF_6^-]^+$), 286.5 (100, $[M - 2PF_6^-]^{2+}$).

[(2,2′-Bipyridine)(2-methylimidazole)(2,2′:6′,2″-terpyridine)-ruthenium(II)] bis(hexafluorophosphate), [Ru(bipy)(terpy)(2-Meimi)](PF$_6$)$_2$, (3). This complex was synthesized using the same procedure as in **2** with 2-methylimidazole (57 mg, 0.7 mmol) and the product was eluted by CH_3OH–CH_2Cl_2 (8% CH_3OH) in the column chromatography. Recrystallization of the dark-brown powder from acetone–EtOH yielded 20 mg (32%) of black crystals. $C_{29}H_{25}N_7RuP_2F_{12}$ (862.56): calc.: C 40.38, H 2.92, N 11.37; found: C, 40.31; H, 2.75; N, 11.17%. ^{1}H NMR: (DMSO-d_6, δ ppm): 12.49 (br s, 1H, NH), 8.98 (d, 1H, J = 8.1 Hz, Ha), 8.84 (d, 2H, J = 8.1, H3′), 8.73 (m, 3H, H3 + e), 8.66 (d, 1H, J = 5.2, Hd), 8.39 (td, 1H, J_1 = 7.8, J_2 = 1.0, Hb), 8.28 (t, 1H, J = 8.1, H4′), 8.11 (td, 2H, J_1 = 7.8, J_2 = 1.1, H4), 7.99–7.89 (m, 2H, Hc + f), 7.84 (d, 2H, J = 5.6, H6), 7.46 (td, 2H, J_1 = 6.1, J_2 = 1.0, H5), 7.27 (d, 1H, J = 4.6, Hh), 7.14 (t, 1H, J = 6.1, Hg), 6.98 (t, 1H, J = 2.0, Hk), 5.62 (s, 1H, Hj), 1.53 (s, 3H, CH_3). ESI-MS: m/z (intensity (%), fragment) 717.9 (73, $[M - PF_6^-]^+$), 604.0 (29, Ru-containing fragment), 572.1 (53, $[M - H^+ - 2PF_6^-]^+$), 521.9 (59, $[Ru(bipy)(terpy)^{2+} - H^+ + CH_3OH]^+$), 490.2 (100, $[Ru(bipy)(terpy)^{2+}–H^+]^+$), 286.4 (92, $[M - 2PF_6^-]^{2+}$).

[(Benzimidazole)(2,2′-bipyridine)(2,2′:6′,2″-terpyridine)ruthenium(II)] bis(hexafluorophosphate), [Ru(bipy)(terpy)(benzimi)](PF$_6$)$_2$, (4). [Ru(bipy)(terpy)Cl]PF_6 (50 mg, 0.074 mmol) was refluxed with benzimidazole (41 mg, 0.35 mmol) in ethanol–H_2O (15 ml/15 ml) for 5 h. The work-up was similar to that of compound **2**. Black crystals were obtained (32 mg, 51%). $C_{32}H_{25}N_7RuP_2F_{12}$ (898.60): calc.: C 42.77, H, 2.80, N 10.91; found: C 42.61, H 2.90, N 10.74%. ^{1}H NMR: (DMSO-d_6, δ ppm): 13.00 (s, 1H, NH), 9.01 (d, 1H, J = 8.3 Hz, Ha), 8.83 (d, 2H, J = 8.0, H3′), 8.75 (m, 4H, H3 + e + d), 8.38 (td, 1H, J_1 = 7.9, J_2 = 1.2, Hb), 8.28 (t, 1H, J = 8.0, H4′), 8.11 (td, 2H, J_1 = 7.8, J_2 = 1.0, H4), 8.01–7.82 (m, 4H, Hc + f + 6), 7.55 –7.46 (m, 3H, H5 + α), 7.35–7.14 (m, 4H, Hh + i + β + γ), 7.02 (td, 1H, J_1 = 7.8, J_2 = 1.2, Hg), 6.86 (d, 1H, J = 8.2, Hδ). ESI-MS: m/z (intensity (%), fragment) 753.8 (28, $[M - PF_6^-]^+$), 608.1 (100, $[M - H^+ - 2PF_6^-]^+$), 490.2 (8, $[Ru(bipy)(terpy)^{2+} - H^+]^+$), 304.3 (13, $[M - 2PF_6^-]^{2+}$).

[(2,2′-Bipyridine)(4,5-diphenylimidazole)(2,2′:6′,2″-terpyridine)ruthenium(II)] bis(hexafluorophosphate), [Ru(bipy)(terpy)-(Ph$_2$imi)](PF$_6$)$_2$, (5). This complex was synthesized and purified by the same procedure as **4** except that 4,5-diphenylimidazole (77 mg, 0.35 mmol) was used instead of benzimidazole. Yield: 37 mg (50%). Black prismatic single crystals were obtained by diffusion of diethyl ether to a methanol solution of the product. This compound crystallizes with one molecule of methanol and analyzed as $C_{40}H_{31}N_7RuP_2F_{12}\cdot CH_3OH$ (1032.77): calc.: C 47.68, H 3.42, N 9.49; found: C 47.13, H 3.49, N 9.61%. ^{1}H NMR: (DMSO-d_6, δ ppm): 13.35 (s, 1H, NH), 9.06 (d, 1H, J = 5.5, Hd), 8.94 (d, 1H, J = 8.0, Ha), 8.65 (d, 3H, J = 8.0, H3 + e), 8.43 (t, 3H, J = 7.4, H3′ + b), 8.25 (t, 2H, J = 8.0, H4), 8.11 (t, 1H, J = 6.5, H4′), 7.92–7.82 (m, 4H, Hc + f + 6), 7.45 (s, 1H, Hi), 7.32 (br s, 2H, H5), 7.12 (m, 5H, Hg + phenyl-4H), 6.95 (d, 1H, J = 6.0, Hh), 6.85 (m, 4H, phenyl), 6.46 (br s, 2H, phenyl), 4.06 (q, 1H, J = 5.4, CH_3OH), 3.18 (d, 3H, J = 5.2, CH_3OH). ESI-MS: m/z (intensity (%), fragment) 855.9 (26, $[M - PF_6^-]^+$), 710.0 (47, $[M - H^+ - 2PF_6^-]^+$), 355.5 (100, $[M - 2PF_6^-]^{2+}$).

[(2,2′-Bipyridine)(indazole)(2,2′:6′,2″-terpyridine)ruthenium-(II)] bis(hexafluorophosphate), [Ru(bipy)(terpy)(inda)](PF$_6$)$_2$, (6). [Ru(bipy)(terpy)Cl]PF_6 (50 mg, 0.074 mmol) was refluxed with an excess of indazole (26 mg, 0.22 mmol) in ethanol–H_2O (12 ml/12 ml) for 5 h. The work-up was similar to that of compound **1**. Yield: 38 mg (60%). Red crystals of X-ray quality were obtained by diffusion of diethyl ether into a methanol solution of the product. $C_{32}H_{25}N_7RuP_2F_{12}$ (898.60): calc.: C 42.77, H 2.80, N 10.91; found: C 42.89, H 2.60, N 10.93%. ^{1}H NMR: (DMSO-d_6, δ ppm): 12.72 (d, 1H, J = 1.4 Hz, NH), 8.98 (d, 1H, J = 8.1, Ha), 8.83 (d, 2H, J = 8.2, H3′), 8.74 (m, 3H, H3 + e), 8.62 (d, 1H, J = 4.7, Hd), 8.38 (td, 1H, J_1 = 7.8, J_2 = 1.3, Hb), 8.30 (t, 1H, J = 8.2, H4′), 8.15 (td, 2H, J_1 = 8.0, J_2 = 1.4, H4), 7.93 (t, 2H, J = 7.2, Hc + f), 7.85 (d, 2H, J = 5.6, H6), 7.59–7.51 (m, 2H, H5 + α), 7.42–7.32 (m, 4H, Hh + i + γ + δ), 7.19 (td, 1H, J_1 = 6.7, J_2 = 1.1, Hg), 7.11 (td, 1H, J_1 = 7.2, J_2 = 1.5, Hβ). ESI-MS: m/z (intensity (%), fragment) 754.1 (5, $[M - PF_6^-]^+$), 608.2 (26, $[M - H^+ - 2PF_6^-]^+$), 490.2 (6, $[Ru(bipy)(terpy)^{2+} - H^+]^+$), 304.6 (100, $[M - 2PF_6^-]^{2+}$) 261.6 (29 $[Ru(bipy)(terpy)^{2+} + CH_3OH]^{2+}$.

[(2,2′-Bipyridine)(pyrazole)(2,2′:6′,2″-terpyridine)ruthenium-(II)] bis(hexafluorophosphate), [Ru(bipy)(terpy)(pyr)](PF$_6$)$_2$, (7). [Ru(bipy)(terpy)Cl]PF_6 (50 mg, 0.074 mmol) and pyrazole (25 mg, 0.35 mmol) were refluxed in ethanol–H_2O (15 ml/15 ml) for 5 h, followed by work-up as described above for **1**. The product was chromatographed (8% CH_3OH in CH_2Cl_2) and recrystallized from acetone–ethanol to yield dark-red crystals (29 mg, 46%). $C_{28}H_{23}N_7RuP_2F_{12}$ (848.54): calc.: C 39.63, H 2.73, N 11.55; found: C 39.63, H 2.66, N 11.88%. ^{1}H NMR: (DMSO-d_6, δ ppm): 12.71 (s, 1H, NH), 8.97 (d, 1H, J = 8.0 Hz, Ha), 8.84 (d, 2H, J = 8.2, H3′), 8.73 (m, 3H, H3 + e), 8.51 (d, 1H, J = 5.2, Hd), 8.40 (t, 1H, J = 8.0, Hb), 8.30 (t, 1H, J = 8.2, H4′), 8.13 (td, 2H, J_1 = 7.8, J_2 = 1.2, H4), 8.10–7.91 (m, 3H, Hc + f + k), 7.80 (d, 2H, J = 5.2, H6), 7.50 (t, 2H, J = 6.5, H5), 7.33 (d, 1H, J = 4.8, Hh), 7.17 (t, 1H, J = 6.5, Hg), 6.66 (s, 1H, Hi), 6.33 (s, 1H, Hj). ESI-MS: m/z (intensity (%), fragment) 703.6 (3, $[M - PF_6^-]^+$), 558.0 (100, $[M - H^+ - 2PF_6^-]^+$),

Table 1 Hydrogen bonding parameters in **5**·CH_3OH and $[Ru(bipy)(terpy)(H_2O)](PF_6)_2$.

D–H···A[a]	D–H/Å	H···A/Å	D···A/Å	D–H···A/°	Sym. rel.
5·CH_3OH					
N7–H7···O	0.87	2.01	2.821(5)	155	
O–H···F7	0.83	2.31	3.019(5)	144	
O–H···F12	0.83	2.43	3.041(5)	131	
$[Ru(bipy)(terpy)(H_2O)](PF_6)_2$					
O–H1···F3	0.85(5)	2.07(5)	2.884(11)	159(8)	3_656[b]
O–H1···F5	0.85(5)	2.20(7)	2.924(10)	143(8)	3_656[b]
O–H2···F1	0.92(5)	1.75(5)	2.652(9)	169(8)	4_566[b]

[a] D = Donor, A = acceptor. [b] Principal symmetry relations (without translation): 3 = $-x, -y, -z$; 4 = $x, -y - 1/2, z - 1/2$.

521.8 (3, $[Ru(bipy)(terpy)^{2+} - H^+ + CH_3OH]^+$), 490.2 (7, $[Ru(bipy)(terpy)^{2+} - H^+]^+$), 279.4 (26, $[M - 2PF_6^-]^{2+}$).

[(2, 2′-Bipyridine)(3-methylpyrazole)(2, 2′ : 6′, 2″-terpyridine)-ruthenium(II)] bis(hexafluorophosphate), [Ru(bipy)(terpy)(3-Mepyr)](PF$_6$)$_2$, (8). This compound was prepared in the same way as **7** by using 3-methylpyrazole (29 mg, 0.35 mmol) instead of pyrazole. Dark-red crystals were obtained (35 mg, 55%). $C_{28}H_{23}N_7RuP_2F_{12}\cdot 2H_2O$ (898.59): calc.: C 38.76, H 3.25, N 10.91; found: C 38.08, H 2.68, N 10.27%. ^{1}H NMR: (DMSO-d_6, δ ppm): 12.35 (s, 1H, NH), 8.96 (d, 1H, J = 7.8 Hz, Ha), 8.83 (d, 2H, J = 8.1, H3′), 8.71 (m, 3H, H3 + e), 8.61 (d, 1H, J = 5.1, Hd), 8.40 (t, 1H, J = 6.7, Hb), 8.29 (t, 1H, J = 8.1, H4′), 8.11 (td, 2H, J_1 = 7.9, J_2 = 1.2, H4), 7.99 (td, 1H, J_1 = 7.0, J_2 = 1.0, Hc), 7.90 (td, 1H, J_1 = 7.9, J_2 = 1.0, Hf), 7.78 (d, 2H, J = 5.3, H6), 7.49 (t, 2H, J = 6.6, H5), 7.29 (d, 1H, J = 4.6, Hh), 7.16 (t, 1H, J = 6.4, Hg), 6.44 (s, 1H, Hj), 6.04 (s, 1H, Hi), 2.14 (s, 3H, CH_3). ESI-MS: m/z (intensity (%), fragment) 718.1 (4, $[M - PF_6^-]^+$), 572.0 (9, $[M - H^+ - 2PF_6^-]^+$), 286.1 (100, $[M - 2PF_6^-]^{2+}$).

[(2,2′-Bipyridine)(cytochrome *c*)(2,2′:6′,2″-terpyridine)ruthenium(II)]$^{2+}$, [Ru(bipy)(terpy)(cyt *c*)]$^{2+}$, (9). A mixture of cytochrome *c* (18.9 mg, 1.5 μmol, Yeast iso-1 cytochrome *c* from Sigma) and $[Ru(bipy)(terpy)(H_2O)](PF_6)_2$ (6.0 mg, 7.5 μmol) was stirred under argon in 2.5 mL of sodium phosphate buffer (μ = 0.1, pH 7.0) for 5 d at 35 °C in the dark. Excess $[Ru(bipy)(terpy)(H_2O)](PF_6)_2$ was removed by passing the solution through a PD-10 desalting column (Sephadex G-25; separates molecules with M < 1000 g mol^{-1}, *i.e.* the unreacted Ru-complex from molecules with M > 5000 g mol^{-1}, *i.e.* the protein and Ru–protein complex). The protein band was loaded on an Econo-Pac CM Ion Exchange Cartridge (BioRad) and purified by FPLC (fast performance liquid chromatography; to separate the Ru-coupled protein from uncoupled cyt *c*) using a linear sodium chloride gradient (Buffer A: 50 mM NaP_i, buffer B: 400 mM NaCl + 25 mM NaP_i, pH 7.0). The band eluting at ~62% buffer B was collected and concentrated using ultrafiltration stirred cells and centricon devices (YM3 and 5000 membranes, respectively) (Yield: 0.13 μmol). The product was identified by absorption, emission and MS measurements (see text).

Structure determinations

X-ray crystallography: *Data collection*: Bruker Smart with CCD area-detector, Mo-Kα radiation (λ = 0.71073 Å), graphite monochromator. Data collection and cell refinement with SMART,[35] data reduction with SAINT,[35] experimental absorption correction with SADABS.[36] *Structure analysis and refinement*: The structures were solved by direct methods (SHELXS-97);[37] refinement was done by full-matrix least squares on F^2 using the SHELXL-97 program suite.[37] All non-hydrogen positions were found and refined with anisotropic temperature factors. Hydrogen atoms on carbon and nitrogen were calculated using appropriate riding models (AFIX 43), U_{eq}(H) = 1.2U_{eq}(C/N). The hydrogen atoms of the methanol molecule in **5**·CH_3OH were calculated with the riding models AFIX 137 (CH_3) and AFIX 147 (OH, d(O–H) = 0.83 Å) and isotropic temperature factors of U_{eq}(H) = 1.5U_{eq}(C/O). The position of the O-bonded H of the methanol molecule was refined with respect to a staggered conformation and an N–H···O and possible O–H···F hydrogen bridge (see Table 1). Hydrogen atoms of the aqua ligand in $[Ru(bipy)(terpy)(H_2O)](PF_6)_2$ were located in the difference map and refined with isotropic displacement parameters U_{eq} = 1.2U_{eq}(O). Also here O–H···F hydrogen bonding is observed with the parameters given in Table 1. In the room-temperature structures of **1** and $[Ru(bipy)(terpy)(H_2O)](PF_6)_2$ the fluorine atoms of the PF_6 anions were disordered. Crystal data are listed in Table 2. Graphics were computed with ORTEP3 for Windows (probability ellipsoids are 50% for the low-temperature and 30% for the room temperature structures).[38] Computations on the supramolecular interactions were carried out with PLATON for Windows.[39]

CCDC reference numbers 251482 (**1**), 251480 (**5**·CH_3OH), 251481 (**6**) and 251479 ($[Ru(bipy)(terpy)(H_2O)](PF_6)_2$).

See http://www.rsc.org/suppdata/dt/b4/b414999h/ for crystallographic data in CIF or other electronic format.

Results and discussion

The $[Ru(bipy)(terpy)L](PF_6)_2$ complexes with L = imidazole, pyrazole and derivatives, were synthesized from $RuCl_3\cdot xH_2O$ *via* $Ru(terpy)Cl_3$ and by refluxing the immediate starting material $[Ru(bipy)(terpy)Cl]PF_6$ with an up to 10-fold excess of the imidazole or pyrazole ligand (eqn. (3)). After precipitating the product complexes by addition of NH_4PF_6, they were separated by column chromatography on silica gel. There was a trace amount of unreacted ruthenium chloride complex, which was eluted first, and the desired products were eluted as the second band. They were then further purified by recrystallization.

$$RuCl_3\cdot xH_2O + terpy \xrightarrow[\text{reflux, 3 h}]{\text{EtOH}} Ru(terpy)Cl_3$$

$$Ru(terpy)Cl_3 + bipy \xrightarrow[\text{2. LiCl, reflux, 0.5 h}]{\text{1. EtOH/H}_2\text{O, reflux, 5 h}} [Ru(bipy)(terpy)Cl]PF_6$$

$$[Ru(bipy)(terpy)Cl]PF_6 + L \xrightarrow[\text{2. NH}_4\text{PF}_6]{\text{1. EtOH/H}_2\text{O, reflux, 5 h}} [Ru(bipy)(terpy)L](PF_6)_2\downarrow \quad (3)$$

(excess)

In the ^{1}H NMR spectra of $[Ru(bipy)(terpy)L]^{2+}$ the two pyridine rings of the bipyridine moiety are nonequivalent, while the terpyridine ligand is split into two equivalent parts by a plane of symmetry (see Scheme 1). This allows for an easy distinction of the terpyridine from the bipyridine protons due to their 2 : 1

Table 2 Crystal data for compounds **1**, **5**, **6** and [Ru(bipy)(terpy)(H_2O)](PF_6)$_2$

Compound	**1**	**5**·CH_3OH	**6**	[Ru(bipy)(terpy)(H_2O)](PF_6)$_2$
Empirical formula	$C_{28}H_{23}F_{12}N_7P_2Ru$	$C_{41}H_{35}F_{12}N_7OP_2Ru$	$C_{32}H_{25}F_{12}N_7P_2Ru$	$C_{25}H_{21}F_{12}N_5OP_2Ru$
M/g mol^{-1}	848.54	1032.77	898.60	798.48
Crystal size/mm	0.25 × 0.20 × 0.10	0.23 × 0.12 × 0.06	0.20 × 0.34 × 0.36	0.20 × 0.15 × 0.05
Crystal description	Isometric	Prismatic	Isometric	Plates
Crystal color	Black	Dark-red to black	Red	Orange–brown
T/K	293(2)	213(2)	223(2)	293(2)
Diffractometer	Bruker Smart 1000	Bruker Smart AXS	Bruker Smart AXS	Bruker Smart 1000
Scan type, 2θ range/°	ϕ and ω, 3.3–50.1	ω, 2.4–50.1	ω, 4.6–53.1	ϕ and ω, 4.5–50.1
h; k; l range	−16, 16; −12, 16; −22, 17	−22, 22; −16, 16; −21, 21	−44, 24; −3, 13; −22, 21	−18, 20; −12, 12; −17, 18
Crystal system	Monoclinic	Monoclinic	Orthorhombic	Monoclinic
Space group	$P2_1/n$	$P2_1/c$	$Pbcn$	$P2_1/c$
a/Å	14.191(5)	18.9571(12)	35.704(3)	16.976(10)
b/Å	13.802(5)	13.7320(9)	10.4729(8)	10.567(6)
c/Å	19.068(6)	17.7831(11)	18.4357(14)	15.275(9)
β/°	99.049(7)	115.765(1)	90	95.938(12)
V/Å^3	3688(2)	4169.1(5)	6893.5(9)	2726(3)
Z	4	4	8	4
D_c/g cm^{-3}	1.528	1.645	1.732	1.946
F(000)	1688	2080	3584	1584
μ/mm^{-1}	0.602	0.551	0.650	0.809
Min./max. transmission	0.8640/0.9422	0.8838/0.9677	0.8045/0.8810	0.8550/0.9607
Measured reflections	14194	30258	22273	10966
Unique reflections (R_{int})	6175 (0.1670)	7394 (0.0497)	6978 (0.0322)	4818 (0.1047)
Obs. refl. [$I > 2\sigma(I)$]	2148	5219	4990	3559
Parameters refined	452	579	487	466
Max./min. $\Delta\rho$/e Å^{-3}[a]	0.646; −0.423	0.935; −1.081	0.698; −0.576	1.233; −1.249
R_1; wR_2[b][$I > 2\sigma(I)$]	0.0814; 0.0959	0.0478; 0.0831	0.0442; 0.1024	0.0702; 0.1450
R_1; wR_2[b](all refl.)	0.1158; 0.2407	0.0790; 0.0973	0.0671; 0.1138	0.0908; 0.1584
Goodness-of-fit[c]	1.179	1.122	1.057	0.920
Weight. scheme w; a/b[d]	0.0000; 0.0000	0.0042; 12.0422	0.0483; 7.6673	0.0000; 3.0741
Extinction coefficient	0.0062(3)	None	None	None

[a] Largest difference peak and hole. [b] $R1 = [\sum(||F_o| - |F_c||)/\sum|F_o|]$; $wR2 = [\sum[w(F_o^2 - F_c^2)^2]/\sum[w(F_o^2)^2]]^{1/2}$. [c] Goodness-of-fit = $[\sum[w(F_o^2 - F_c^2)^2]/(n-p)]^{1/2}$. [d] $w = 1/[\sigma^2(F_o^2) + (aP)^2 + bP]$ where $P = (\max(F_o^2 \text{ or } 0) + 2F_c^2)/3$.

integral ratio. In the precursor [Ru(bipy)(terpy)Cl]$^+$ the proton of the bipyridine ligand, which is closest to the chloride ion (Hd in Scheme 1), has a quite low-field chemical shift (~10.2 ppm) with respect to the other bipy protons.[21] Upon substitution of the Cl^--ion by other ligands L this proton is shifted upfield because of the larger diamagnetic anisotropy of these ligands over Cl^-.[40] In [Ru(bipy)(terpy)L]$^{2+}$ (**1–8**) the chemical shift of Hd (bipy) lies in the range of 8.5–9.1 ppm. The assignment of the ^{1}H NMR spectra of the complexes reported here was accomplished from the integral ratio, the upfield shift of Hd, as well as by H,H COSY spectroscopy. As an example, the ^{1}H NMR and H,H COSY of the imidazole complex **1** is illustrated in Fig. 1.

ESI-mass spectra of the complexes show good consistence with the corresponding formula (see Experimental section). In general, a singly positively charged ion appeared at the largest m/z value, which resulted from the loss of one hexafluorophosphate anion with formation of a [[Ru(bipy)(terpy)L](PF_6)]$^+$ cation. The most intensive fragment is due to the doubly charged cation [Ru(bipy)(terpy)L]$^{2+}$. The singly charged cation of [Ru(bipy)(terpy)L − H^+]$^+$ and, in some cases, the fragment of [Ru(bipy)(terpy) − H^+]$^+$ (m/z = 490), can also be found in the mass spectra.[42]

X-Ray structures have been determined for complexes **1**, **5**·CH_3OH and **6** as models of the histidine-protein binding to the [Ru(bipy)(terpy)]$^{2+}$ moiety and for the synthetically important aqua complex [Ru(bipy)(terpy)(H_2O)](PF_6)$_2$. ORTEP drawings of the cations of these complexes are shown in Figs. 2–5; selected bond lengths and bond angles are collected in Table 3.

In the structures of [Ru(bipy)(terpy)L]$^{2+}$ the ruthenium(II) ion is coordinated by a tridentate terpyridine, a bidentate bipyridine and a monodentate imidazole or indazole ligand in a distorted octahedral geometry. The terpy ligand is planar or slightly twisted (in the case of complex **5**) and coordinates in *mer* fashion while the bipy ligand is planar. The monodentate ligand L is necessarily *trans* to one of the bipyridine nitrogen atoms.

In each compound the bond distance of ruthenium to the central pyridyl nitrogen atom of the terpy ligand, (Ru–N2) is significantly shorter than those to the outer pyridyl rings (Ru–N1 and Ru–N3) or to the bipy and L nitrogen atoms (Ru–N4,5,6). This shortening of the Ru–N2 bond length by approximately 0.1 Å, together with the N1–Ru–N3 angles of around 159°, are typical features of the coordination of a terpy ligand to ruthenium or osmium and have been reported in a number of examples.[16,18,19,21,43–47]

The bond distances from ruthenium to the two bipyridine nitrogen atoms within each complex are slightly different, with the longer bond *trans* to the central pyridyl of the terpy ligand and *cis* to L or H_2O. Conversely, the Ru–N_{bipy} bond *trans* to the ligand L or H_2O is the shorter one. This is also typical for [Ru(bipy)(terpy)L]$^{2+}$ complexes and was explained by interligand steric interactions rather than a *trans* effect of the central nitrogen of the terpy ligand.[16]

The Ru–N6 bond lengths to the mono-dentate ligand L are similar to the bond lengths Ru–N5 of the *cis*-coordinated bipy moiety. The imidazole or indazole plane is roughly perpendicular to the plane defined by the terpy ligand. The steric hindrance of the two phenyl groups in the diphenylimidazole ligand in **5** results in slightly longer Ru–N distances to most nitrogen atoms in comparison to complexes **1** and **6**. Most bond angles in **5** also differ from those of the other two complexes.

Despite the presence of ligand π-systems in the cations of compounds **1**, **5**, **6** and [Ru(bipy)(terpy)(H_2O)](PF_6)$_2$ there are only few intermolecular C–H $\cdots$ π[48] or π–π interactions[49] evident, due to the separating action of the PF_6-anions. These few non-covalent π-stacking interactions can be viewed as medium to weak in that they exhibit rather long centroid–centroid distances (>4.0 Å) together with large slip angles (β, γ > 30°) and vertical displacements (a > 2.0 Å) between the ring centroids.[50] The C–H $\cdots$ π contacts lie at the short end of the accepted distance range for this type of contact.[48,51] The cation of compound **5**

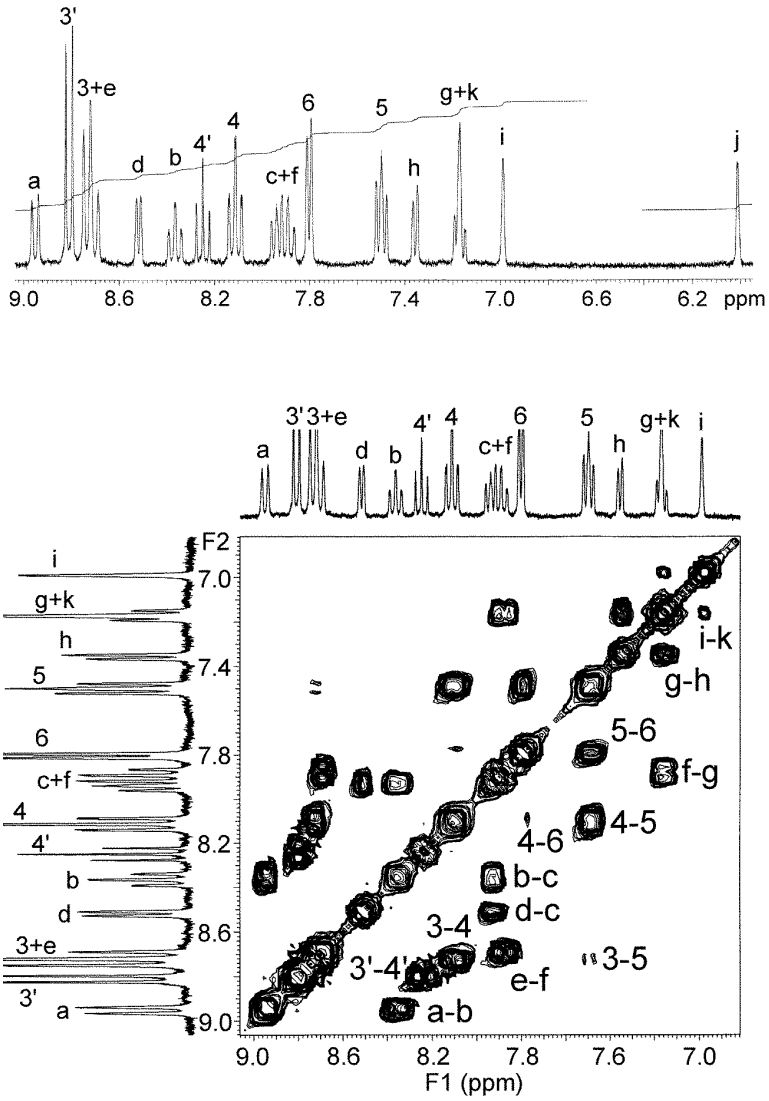

Fig. 1 ^{1}H NMR spectrum and H,H-COSY of compound **1** (L = imi); for the numbering assignment see Scheme 1. The imidazole protons appear at higher field at 7.00 and 6.02 ppm for Hi and Hj of the imidazole ring; Hk is overlapped with Hg at 7.18 ppm as a triplet.[41]

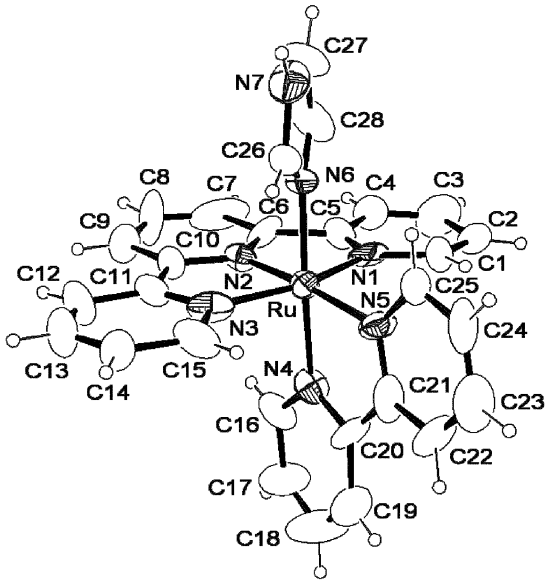

Fig. 2 Molecular structure of the [Ru(bipy)(terpy)(imi)]$^{2+}$ cation in **1**.

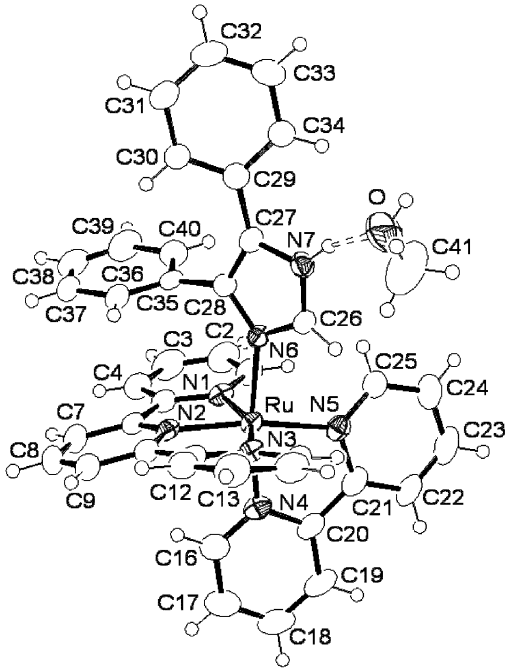

Fig. 3 Molecular structure of the [Ru(bipy)(terpy)(Ph$_2$imi)]$^{2+}$cation together with the hydrogen-bonded methanol molecule in **5**·CH$_3$OH. The atom numbers of the unlabeled atoms are the same as in Fig. 2.

also features intramolecular π–π stacking between one of the phenyl groups of the imidazole ligand and the terpyridine ligand (see Fig. 3). There is also substantial intramolecular π-overlap

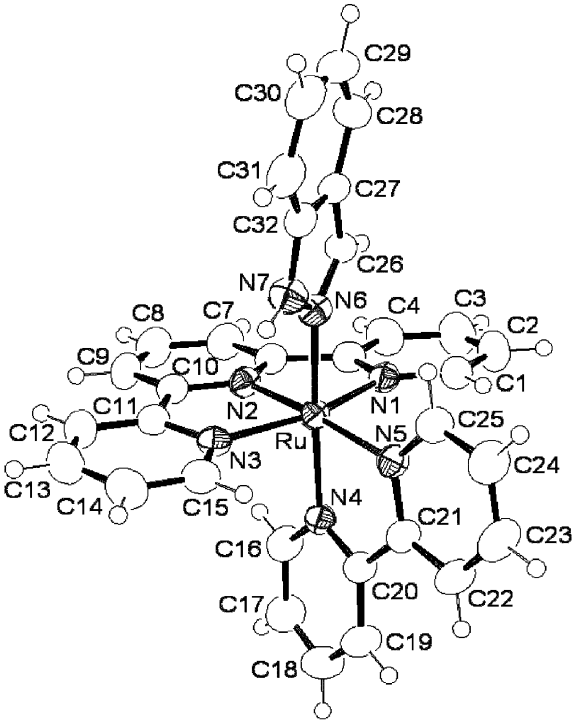

Fig. 4 Molecular structure of the $[Ru(bipy)(terpy)(inda)]^{2+}$ cation in **6**.

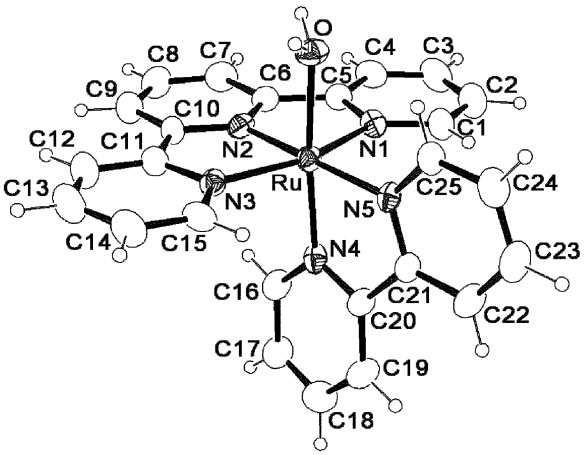

Fig. 5 Molecular structure of the $[Ru(bipy)(terpy)(H_2O)]^{2+}$ cation in $[Ru(bipy)(terpy)(H_2O)](PF_6)_2$.

between this phenyl ring plane and the metal chelate ring built from Ru–N1–N2–C5–C6. It has been suggested that an active electron delocalization within the metal-N-heterocyclic chelate ring could exhibit some degree of "metalloaromaticity".[52,53] The possibility of the hydrophobic $[Ru(bipy)(terpy)]^{2+}$-fragment to enter into C–H $\cdots$ π or π-stacking interactions with the hydrophobic grooves of the protein may be an additional aspect of its protein binding.[54]

UV/Vis spectroscopy: The absorption spectra of complexes **1–8** and the starting materials $[Ru(bipy)(terpy)Cl]PF_6$ and $[Ru(bipy)(terpy)(H_2O)](PF_6)_2$ have been measured in acetonitrile and, in order to have the similar conditions present during protein coupling, in aqueous solution. Table 4 summarizes the absorption bands together with the extinction coefficients and Fig. 6 shows some selected spectra of the complexes.

In all cases the UV/Vis spectra show a broadened, unresolved band in the 400–600 nm range which is due to the metal-to-ligand charge transfer [MLCT, d(Ru)–π*(terpy or bipy)].[2] The maxima of this band vary a little among the complexes, and are centered around 475 nm for the imidazole-based compounds **1–5** and at around 460 nm for the pyrazole-based compounds **6–8**.

Table 3 Selected bond distances (Å) and bond angles (°).

Compound	**1**	**5**·CH_3OH	**6**	Ru–H_2O
Ru–N1	2.006(10)	2.071(3)	2.068(3)	2.010(6)
Ru–N2	1.916(9)	1.957(3)	1.968(3)	1.909(6)
Ru–N3	2.015(10)	2.082(3)	2.068(3)	2.020(6)
Ru–N4	2.042(8)	2.072(4)	2.055(3)	1.969(6)
Ru–N5	2.085(8)	2.100(4)	2.080(3)	1.991(6)
Ru–N6	2.072(8)	2.124(3)	2.086(3)	
Ru–O				2.097(5)
N1–Ru–N2	79.0(4)	79.7(2)	79.8(1)	80.4(3)
N1–Ru–N3	158.4(4)	159.1(2)	159.5(1)	159.7(3)
N1–Ru–N4	91.9(3)	93.5(2)	92.9(1)	93.1(3)
N1–Ru–N5	101.5(4)	96.8(2)	99.8(1)	96.6(3)
N1–Ru–N6	90.9(4)	94.42(2)	90.4(1)	
N1–Ru–O				89.0(2)
N2–Ru–N3	79.4(4)	79.5(2)	79.7(1)	79.3(3)
N2–Ru–N4	96.1(3)	91.8(2)	95.2(1)	98.3(2)
N2–Ru–N5	174.8(4)	169.3(2)	173.8(1)	176.4(3)
N2–Ru–N6	89.6(3)	95.1(2)	91.8(1)	
N2–Ru–O				89.8(2)
N3–Ru–N4	89.2(3)	89.9(2)	88.7(1)	90.0(2)
N3–Ru–N5	100.0(4)	104.1(2)	100.6(1)	103.7(2)
N3–Ru–N6	90.1(4)	84.7(2)	90.5(1)	
N3–Ru–O				90.7(2)
N4–Ru–N5	78.7(4)	78.2(2)	78.6(1)	79.7(2)
N4–Ru–N6	174.0(4)	170.3(2)	172.7(1)	
N4–Ru–O				171.8(2)
N5–Ru–N6	95.6(4)	95.3(2)	94.4(1)	
N5–Ru–O				92.2(2)

No distinguishable shoulders which would indicate any energy differences of the d–π*(terpy) or d–π*(bipy) charge transfer are observed in this range, different from what has been reported for the $[Ru(bipy)(terpy)(py)]^{2+}$ and $[Ru(bipy)(terpy)(CH_3CN)]^{2+}$ complexes.[16] Only a very poorly resolved shoulder can be found around 410 nm in the spectra of complexes **1–5**. The chloro-complex, $[Ru(bipy)(terpy)Cl]^+$ has a red-shifted MLCT band at 503 nm in acetonitrile solution, but it changes to 474 nm when measured in H_2O. Although this band appears slightly sensitive to the solvent,[2] a comparison with the UV/Vis spectrum of the aqua analog $[Ru(bipy)(terpy)(H_2O)]^{2+}$ (λ_{max} 476 nm in H_2O) suggests that the Cl-ligand is actually replaced by H_2O in aqueous solution to form the $[Ru(bipy)(terpy)(H_2O)]^{2+}$ complex.

At the short wavelength side of the spectra, all the complexes show absorption bands at 230 and 288 nm (with two more or less resolved shoulders at 272 and 279 nm) which are assigned to the ligand centered (LC) π–π* transitions of the bipy or terpy ligands. A further band at 310 nm might be the MC (metal centered) transition.[2]

Emission spectra: The emission spectra were also measured in acetonitrile and water solutions at room temperature. Upon excitation at 475 nm, where the MLCT bands appear, complexes **1** and **2** show emission at around 660 nm (Fig. 7). Under the same experimental conditions, no signals or only very weak emission were observed for the other complexes, **3–8**, and the chloro- and aqua-complexes in the region of 500–800 nm. This feature is interesting for monitoring the protein binding (see below). The imidazole complex $[Ru(bipy)(terpy)(imi)]^{2+}$ (**1**) has an emission peak at 662 nm which has also been observed in the bipy analog $[Ru(bipy)_2(im)_2]^{2+}$,[55] and which has been applied in the monitoring of protein modification reactions.[7] The 4-methylimidazole derivative, $[Ru(bipy)(terpy)(4\text{-}Meimi)]^{2+}$ (**2**) exhibits similar emission properties to **1** with a maximum slightly red-shifted to 667 nm (Fig. 7), whilst the 2-methylimidazole complex **3** shows a very weak peak (see also Fig. 7) and the benzimidazole and 4,5-diphenylimidazole complexes **4** and **5** have no detectable fluorescence. These results suggest that emission spectroscopy can be used in the analysis of the modification of proteins such as cytochrome *c* by $[Ru(bipy)(terpy)(H_2O)]^{2+}$. As mentioned above, in such cases the protein is coordinated to

Table 4 Absorption and emission bands of [Ru(bipy)(terpy)Cl]PF_6 (Ru–Cl), [Ru(bipy)(terpy)$(H_2O)](PF_6)_2$ (Ru–H_2O) and complexes **1–8**.[a]

Complex	λ^{abs}/nm ($10^{-4}\varepsilon$/cm^{-1} L^{-1} mol) in acetonitrile					λ^{abs}/nm ($10^{-4}\varepsilon$/cm^{-1} L^{-1} mol) in H_2O				
	π–π^*		MC	MLCT	λ^{em}/nm[c]	π–π^*		MC	MLCT	λ^{em}/nm[c]
Ru–Cl	240 (3.06)	281 (3.37)	293 (3.90)	316 (3.46)	503 (1.02)	No signal	232[b] (2.84)	272[b] sh (3.44)	288[b] (4.00)	312[b] (3.89)	474[b] (1.05)	No signal
Ru–H_2O						No signal	272 sh (2.06)	280 sh (2.17)	288 (2.43)	312 (2.31)	476 (0.61)	No signal
1	233 (3.34)	272 sh (3.73)	289 (4.41)	312 (4.26)	476 (1.03)	660	234 (3.25)		288 (4.27)	312 (4.12)	476 (1.04)	662
2	234 (2.03)	272 (2.87)	290 (3.39)	312 (3.22)	474 (0.76)	667	230 (3.12)	272 sh (2.44)	288 (2.75)	312 (2.73)	476 (0.67)	667
3	232 (2.23)	272 (3.20)	289 (3.63)	313 (3.58)	476 (0.90)	669	230 (3.62)		288 (4.41)	312 (4.36)	475 (1.12)	669
4	230 (3.10)	280 (4.02)	289 (3.91)	314 (3.52)	480 (0.88)	No signal	228 (3.48)		288 (3.82)	313 (3.36)	476 (0.89)	No signal
5	240 (2.65)		289 (3.91)	314 (2.98)	474 (0.76)	No signal	230 (3.46)		288 (4.27)	314 (3.12)	476 (0.62)	No signal
6	229 (2.88)		288 (4.99)	308 (4.22)	458 (0.97)	No signal	230 (1.88)		285 (2.94)	310 (2.54)	463 (0.68)	No signal
7	234 (2.41)		288 (3.80)	312 (3.48)	464 (0.78)	No signal	236 (2.94)		286 (3.86)	310 (3.71)	467 (0.88)	No signal
8	241 (2.28)		286 (4.07)	308 (3.57)	459 (0.91)	No signal	233 (2.69)		288 (3.63)	312 (3.43)	472 (0.88)	No signal

[a] Concentrations 2· $\times 10^{-5}$ mol/L. [b] Assumed to be the Ru–H_2O complex [Ru(bipy)(terpy)$(H_2O)]^{2+}$. [c] Excitation wavelength 475 nm.

Fig. 6 UV/Vis spectra of complexes **1** and **7** in H_2O; the concentrations are 2×10^{-5} mol L^{-1}.

Fig. 7 Emission spectra of complexes **1**, **2** and **3** at concentrations of 2×10^{-5} mol L^{-1}: (a) in CH_3CN, (b) in H_2O. The excitation wavelength λ_{exc} is 475 nm. The fluorescence yield is normalized to the maximum emission in (b).

the metal center through the imidazole nitrogen of the histidine residue which then forms [Ru(bipy)(terpy)({His-}cyt *c*)]$^{2+}$ (in histidine the peptide backbone is attached to the 4-position of imidazole *via* a CH_2 group).

In order to optimize the reaction conditions for protein binding to [Ru(bipy)(terpy)]$^{2+}$, we have studied the substitution of the aqua ligand by imidazole (eqn. (4)) at different pH values (range 5.0–9.0) as a model reaction by following the increase in emission intensity.

$$[Ru(bipy)(terpy)H_2O]^{2+} + imi \xrightarrow{r.t.} [Ru(bipy)(terpy)(imi)]^{2+} + H_2O \quad (4)$$

In the incubation period the concentration of both reactants was 5×10^{-3} mol L^{-1}. Each emission spectrum was measured by diluting a small amount of the reaction mixture to 3.5×10^{-5} mol L^{-1} just prior to the measurement. As shown in Fig. 8(a), at pH 8.5 the fluorescence intensity increased much faster than at other pH values, indicating a higher reaction rate. The intensity reached the maximum after a reaction time of 3 weeks (Fig. 8(b)). The pH dependence is explained by the protonation of imidazole ($pK_S = 7.17$) at lower pH values which decreases the formation of the Ru–imi compounds. At higher pH the Ru–H_2O complex is deprotonated to $[Ru(bipy)(terpy)(OH)]^+$ which will also decrease the reaction rate.

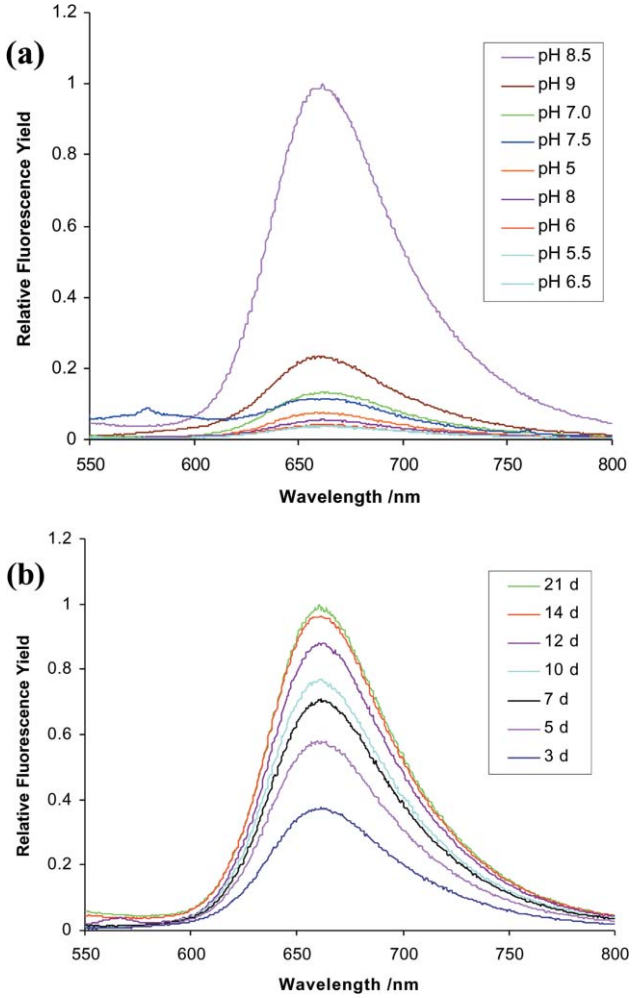

Fig. 8 Emission spectra of the reaction mixture according to eqn. (4) (a) at different pH values after 14 days. The order of the pH-values in the legend follows the order of the intensity at the emission maximum at 662 nm (the curves at pH 5.5 and 6.5 are lying almost on top of each other). (b) At pH 8.5 after 3, 5, 7, 10, 12, 14 and 21 days. Intensity at mission maximum increases with the number of days. The excitation wavelength λ_{exc} is 475 nm; concentrations are 3.5×10^{-5} mol L^{-1}.

Following the results of the pH dependence of the reaction rate for eqn. (4), the protein coupling of $[Ru(bipy)(terpy)(H_2O)]^{2+}$ with cytochrome *c* was first carried out at room temperature in a sodium phosphate buffer of pH 8.5. However, after several days there was no observable change of the reaction mixture which was monitored by UV/Vis and emission spectroscopy. With fresh reagents the temperature was then raised to 35 °C and this time again no desired product was obtained but rather some by-products. Finally, the reaction was done at 35 °C and pH 7.0 for 5 days under argon (eqn. (5)). The fluorescence spectrum of the product (Fig. 9) showed a strong emission at 660 nm upon excitation at 475 nm, which is similar to the Ru–imidazole and –4-methylimidazole complexes **1** and **2** (see Fig. 7), indicating the formation of the Ru–cyt *c* adduct.

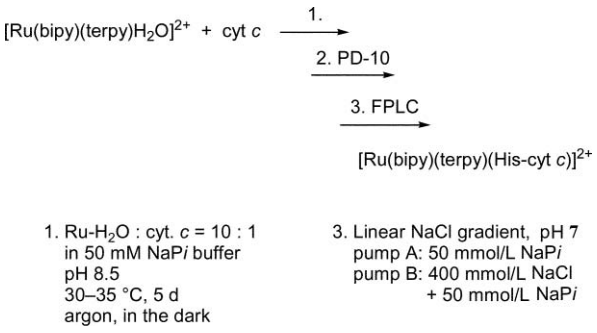

(5)

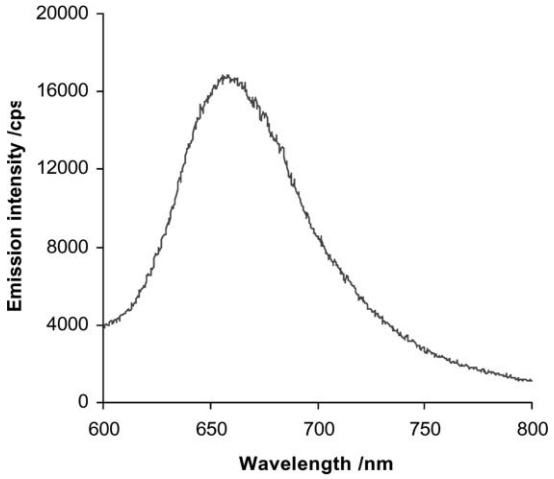

Fig. 9 Emission spectrum of the [Ru(bipy)(terpy)(cyt *c*)]-product according to eqn. (5); excitation wavelength $\lambda_{exc} = 475$ nm, solvent water.

Fig. 10 shows the absorption spectrum of the Ru-modified protein together with those of $[Ru(bipy)(terpy)(H_2O)]^{2+}$ and cyt *c*. The UV/Vis spectrum of the [Ru(bipy)(terpy)(cyt *c*)]-product (Fig. 10) shows absorption bands at 283, 315, 357, 409 and 525 nm. The broadened band at 283 nm is assigned to the LC π–π* transitions of the bipy and terpy ligands, which appears at 288 nm with two shoulders at 272 and 279 nm in the case of the starting $[Ru(bipy)(terpy)(H_2O)]^{2+}$ complex. The MC (metal centered) transition (315 nm) is weakened compared to the Ru–H_2O complex (312 nm). The bands at 357, 409 and 525 nm are typical for oxidized cyt *c*. The metal-to-ligand charge transfer [MLCT, d(Ru)-π*(terpy or bipy)] of the $[Ru(bipy)(terpy)(H_2O)]^{2+}$ complex (476 nm) cannot be resolved in the spectrum due to its much lower ε value than that of cyt *c* at 410 nm. The band at 525 nm and the absence of a band at 550 nm in the spectrum of Ru-modified cyt *c* indicate that it is almost fully oxidized (96%) whereas the spectrum of cyt *c* shows a small amplitude of the band at 550 nm indicating a partially oxidized heme (74%).[56] A stoichiometry of ~0.8 $[Ru(bipy)(terpy))]^{2+}$ per cyt *c* was estimated by a Factor analysis of the UV/Vis spectra

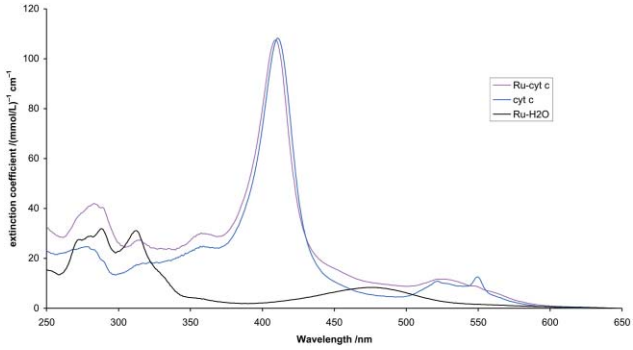

Fig. 10 UV/Vis spectra of $[Ru(bipy)(terpy)(cyt\ c)]^{2+}$, cyt *c* and $[Ru(bipy)(terpy)(H_2O)]^{2+}$ in water.

Table 5 Peptides identified by HPLC-MS after tryptic digestion of [Ru(bipy)(terpy)] coupled to cyt *c*.

Peptide[a]					
Sequence	Position	t_R[b]/min	Calc. mass[c]/Da	Obs. mass[c]/Da	Modification[d]
TEFK	1–4	6.42	523.264	523.263	
AGSAK	5–9	6.32	432.233	432.232	
KGATLFK	10–16	8.88	763.459	763.461	
GATLFK	11–16	10.24	635.364	635.369	
CLQCHTVEK	19–27	16.83	1673.666	1673.688	Heme(Fe^{III})$^+$
GGPHK	28–32	7.61	494.260	494.262	
VGPNLHGIFGR	33–43	14.35	1165.636	1165.640	
HSGQAEGYSYTDANIK	44–59	10.38	1739.775	1739.783	
HSGQAEGYSYTDANIK	44–59	12.79	2224.846	2224.864	Ru^{II}(bipy)(terpy)$^{2+}$
NVLWDENNMSEYLTNPKK	61–78	16.83	2236.083	2236.097	Trimethyllysine
YIPGTK	79–84	8.26	677.375	677.378	
MAFGGLK	85–91	11.90	722.379	722.381	
EKDR	93–96	6.32	546.276	546.274	
NDLITYLK	97–104	14.15	978.539	978.542	

[a] Sequence information from Entry CYC1_YEAST of the Uniprot/Swissprot database.[57] [b] Retention time from HPLC column. [c] Monoisotopic masses of neutral peptides. [d] Modifications identified by peptide mapping and MS/MS fragment spectra.

using reference spectra of oxidized and reduced cyt *c* and that of the [Ru(bipy)(terpy)(H_2O)]$^{2+}$ complex.

A mass spectrum of the Ru-coupled protein product yielded an average neutral mass of 13196.35 Da being close to the calculated mass of 13196.72 Da based on the sum of mass values calculated for cyt *c* (12708.22 Da) and for [Ru(bipy)(terpy)]$^{2+}$ (490.52 Da) minus two protons accounting for the two positive charges of the Ru complex. In addition signals with average masses of 12708.08 and 13058.38 Da could be detected which are attributed to some uncoupled cyt *c* and a cyt *c* carrying an unknown modification, respectively, which have not been completely separated by FPLC. The latter modification can be tentatively attributed to a [Ru(terpy)(H_2O)]$^{2+}$ (average mass = 352.35 Da) coupled to two adjacent histidine side chains at the surface of cyt *c* (His31 and His38). After digestion by trypsin no peptide with a stable mass shift in this range could be identified suggesting that this complex may be unstable in the denatured form of the protein (see also Table 5).

The location where the [Ru(bipy)(terpy)] complex was coupled to the protein was identified using digestion of the Ru-coupled protein by trypsin (cutting C-terminal to Lys and Arg) and analysis by HPLC-MS. Table 5 summarizes the results from peptide mapping. All predicted peptides have been found except two small (Thr-Arg at position 17–18 and Ala-Cys-Glu at the C-terminus) peptides (see Table 5). Fig. 11 shows the ESI-MS spectrum of tryptic peptide 44–59 carrying the [Ru(bipy)(terpy)]

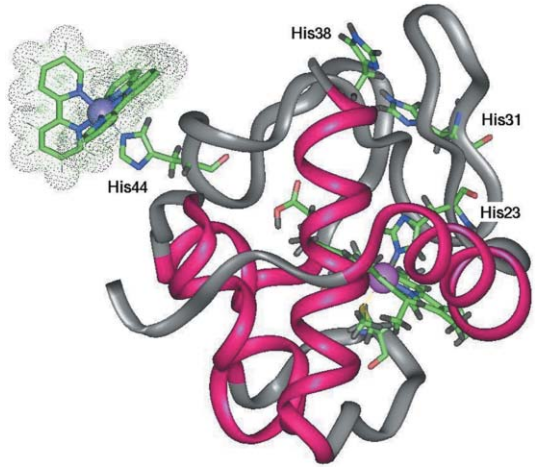

Fig. 12 Molecular model of [Ru(bipy)(terpy)]$^{2+}$ coupled to His44 of cyt *c*. The imidazole ligand of [Ru(bipy)(terpy)(imi)] (*cf*. Fig. 2) was superimposed with the His sidechain of Yeast iso-1 cyt *c* (1YCC.PDB)[58] using the program InsightII (Accelrys).

at His44 (corresponding to His39 in the numbering scheme used in refs. 5*a*, 9*b* and others). The isotopic pattern (see inset of Fig. 11) is indicative of ruthenium. No modifications could be detected for the three other histidines at positions 23 (ligand

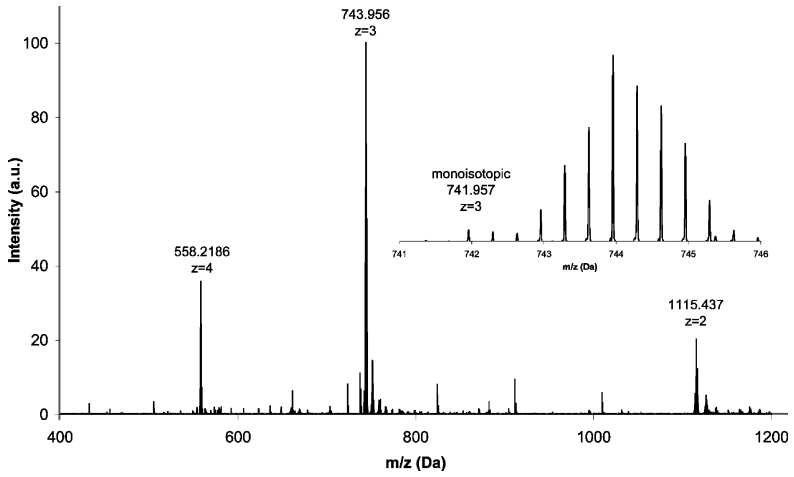

Fig. 11 ESI-MS spectrum at HPLC Ret. Time of 12.79 min containing [Ru(bipy)(terpy)]$^{2+}$ coupled to tryptic peptide [44–59] of cyt *c* at His44. Mass/charge ratios for the highest peaks of the isotope pattern and charges are indicated. Inset: Isotopic pattern of the MH^{3+} ion with monoisotopic mass indicated.

to heme iron), 31 and 38. Fig. 12 illustrates the binding of $[Ru(bipy)(terpy)]^{2+}$ to His44 of Yeast iso-1 cytochrome *c*.

Acknowledgements

This work was supported by the Fonds der Chemischen Industrie and the Universität Freiburg and by the DFG grant to WH (HA 1084/9-1).

References

1 K. Kalyanasundaram, *Coord. Chem. Rev.*, 1982, **46**, 159.
2 A. Juris, V. Balzani, F. Barigelletti, S. Campagna, P. Belser and A. von Zelewsky, *Coord. Chem. Rev.*, 1988, **84**, 85.
3 E. Krausz and J. Ferguson, *Prog. Inorg. Chem.*, 1989, **37**, 293.
4 (*a*) Recent examples:A. C. Benniston, V. Grosshenny, A. Harriman and R. Ziessel, *Dalton Trans.*, 2004, 1227; (*b*) P. Thornton, *Annu. Rep. Prog. Chem., Sect. A*, 2003, **99**, 243; (*c*) J. Slinker, D. Bernards, P. L. Houston, H. D. Abruña, S. Bernhard and G. G. Malliaras, *Chem. Commun.*, 2003, 2392; (*d*) C. Goze, J.-C. Chambron, V. Heitz, D. Pomeranc, X. J. Salom-Roig, J.-P. Sauvage, A. F. Morales and F. Barigelletti, *Eur. J. Inorg. Chem.*, 2003, 3752; (*e*) P. Thornton, *Annu. Rep. Prog. Chem., Sect. A*, 2002, **98**, 235; (*f*) M. I. J. Polson, N. J. Taylor and G. S. Hanan, *Chem. Commun.*, 2002, 1356; (*g*) M. Pauly, I. Kayser, M. Schmitz, M. Dicato, A. Del Guerzo, I. Kolber, C. Moucheron and A. Kirsch-De Mesmaeker, *Chem. Commun.*, 2002, 1086; (*h*) P. Thornton, *Annu. Rep. Prog. Chem., Sect. A*, 2001, **97**, 239; (*i*) P. Thornton, *Annu. Rep. Prog. Chem., Sect. A*, 2000, **96**, 279; (*j*) R. C. Sadoski, G. Engstrom, H. Tian, L. Zhang, C.-A. Yu, L. Yu, B. Durham and F. Millett, *Biochemistry*, 2000, **39**, 4231; (*k*) D. Burdinski, E. Bothe and K. Wieghardt, *Inorg. Chem.*, 2000, **39**, 105.
5 (*a*) J. R. Winkler and H. B. Gray, *Chem. Rev.*, 1992, **92**, 369; (*b*) S. S. Isied, M. Y. Ogawa and J. F. Wishart, *Chem. Rev.*, 1992, **92**, 381; (*c*) S. S. Isied, in Electron Transfer in Biology and the Solid State, Inorganic Compounds with Unusual Properties, *Advances in Chemistry*, ed. M. K. Johnson, R. V. King, D. M. Jr. Kurtz, G. Kutal, M. L. Norton and R. A. Scott, American Chemical Society, Washington, DC, 1990, vol. 226, p. 91; (*d*) F. Millet, in *Metal Ions in Biological Systems*, ed. H. Sigel and A. Sigel, Marcel Dekker, New York, 1991, p. 223; (*e*) J. R. Scott, M. McLean, S. G. Sligar, B. Durham and F. Millett, *J. Am. Chem. Soc.*, 1994, **116**, 7356; (*f*) J. R. Scott, A. Willie, M. McLean, R. S. Stayton, S. G. Sligar, B. Durham and F. Millett, *J. Am. Chem. Soc.*, 1993, **115**, 6820; (*g*) R. Langen, I. Chang, J. P. Germanas, J. H. Richards, J. R. Winkler and H. B. Gray, *Science*, 1995, **268**, 1733; (*h*) F. Millett, M. A. Miller, L. Green and B. Durham, *J. Bioenerg. Biomembranes*, 1995, **27**, 341; (*i*) B. Durham, J. L. Fairris, M. McLean, F. Millett, J. R. Scott, S. G. Sligar and A. Willie, *J. Bioenerg. Biomembranes*, 1995, **27**, 331; (*j*) F. Millett and B. Durham, *Biochemistry*, 2002, **41**, 11315.
6 (*a*) L. Geren, S. Hahm, B. Durham and F. Millett, *Biochemistry*, 1991, **30**, 9450; (*b*) A. Willie, M. McLean, R. Lieu, S. Hilgen-Willis, A. J. Aunders, G. J. Pielak, S. G. Sligar, B. Durham and F. Millett, *Biochemistry*, 1993, **32**, 7519; (*c*) G. Engstrom, R. Rajagukguk, A. J. Saunders, C. N. Patel, S. Rajagukguk, T. Merbitz-Zahradnik, K. Xiao, G. J. Pielak, B. Trumpower, C.-A. Yu, L. Yu, B. Durham and F. Millett, *Biochemistry*, 2003, **42**, 2816.
7 B. Durham, L. P. Pan, S. Hahm, J. Long and F. Millett, in Electron Transfer in Biology and the Solid State, Inorganic Compounds with Unusual Properties, ed. M. K. Johnson, R. V. King, D. M. Jr. Kurtz, G. Kutal, M. L. Norton and R. A. Scott, *Advances in Chemistry*, American Chemical Society, Washington, DC, 1990, vol. 226, p. 181.
8 H. K. Rau, N. DeJonge and W. Haehnel, *Proc. Natl. Acad. Sci. USA*, 1998, **95**, 11526.
9 (*a*) Cytochrome c: D. R. Casimiro, J. H. Richards, J. R. Winkler and H. B. Gray, *J. Phys. Chem.*, 1993, **97**, 13073; (*b*) G. A. Mines, M. J. Bjerrum, M. G. Hill, D. R. Casimiro, I.-J. Chang, J. R. Winkler and H. B. Gray, *J. Am. Chem. Soc.*, 1996, **118**, 1961; (*c*) L. G. Arnaut and S. J. Formosinho, *J. Photochem Photobiol. A: Chem.*, 1998, **118**, 173; (*d*) J. Luo, K. B. Reddy, A. S. Salameh, J. F. Wishart and S. S. Isied, *Inorg. Chem.*, 2000, **39**, 2321; (*e*) and azurin: M. J. Bjerrum, D. R. Casimiro, I-Jy Chang, A. J. Di Bilio, H. B. Gray, M. G. Hill, R. Langen, G. A. Mines, L. K. Skov, J. R. Winkler and D. S. Wuttke, *J. Bioenerg. Biomembranes*, 1995, **27**, 295.
10 (*a*) Synthetic metalloprotein: L. Christian, P. Piotrowiak and R. S. Farid, *J. Am. Chem. Soc.*, 2003, **125**, 11814; (*b*) HiPIPs: E. Babini, I. Bertini, M. Borsari, F. Capozzi, C. Luchinat, X. Zhang, G. L. C. Moura, I. V. Kurnikov, D. N. Beratan, A. Ponce, A. J. Di Bilio, J. R. Winkler and H. B. Gray, *J. Am. Chem. Soc.*, 2000, **122**, 4532; (*c*) plastocyanin: K. Sigfridsson, M. Ejdebäck, M. Sundahl and Ö. Hansson, *Arch. Biochem. Biophys.*, 1998, **351**, 197; (*d*) azurin: A. J. Bi Bilio, M. G. Hill, N. Bonander, B. G. Karlsson, R. M. Villahermosa, B. G. Malmström, J. R. Winkler and H. B. Gray, *J. Am. Chem. Soc.*, 1997, **119**, 9921; (*e*) α-helical peptide: B. I. Dahiyat, T. J. Meade and S. L. Mayo, *Inorg. Chim. Acta*, 1996, **243**, 207.
11 (*a*) See, for example: B. Whittle, N. S. Everest, C. Howard and M. D. Ward, *Inorg. Chem.*, 1995, **34**, 2025; (*b*) N. Grover, N. Gupta, P. Singh and H. H. Thorp, *Inorg. Chem.*, 1992, **31**, 2014; (*c*) J. R. Kirchoff, D. R. McMillin, P. A. Marnot and J.-P. Sauvage, *J. Am. Chem. Soc.*, 1985, **107**, 1138; (*d*) K. D. Demadis, T. J. Meyer and P. S. White, *Inorg. Chem.*, 1997, **36**, 5678; (*e*) M. H. V. Huynh, P. S. White and T. J. Meyer, *J. Am. Chem. Soc.*, 2001, **123**, 9170; (*f*) H. Hofmeier, P. R. Andres, R. Hoogenboom, E. Herdtweck and U. S. Schubert, *Aust. J. Chem.*, 2004, **57**, 419; (*g*) N. Chanda, S. M. Mobin, V. G. Puranik, A. Datta, M. Niemeyer and G. K. Lahiri, *Inorg. Chem.*, 2004, **43**, 1056.
12 H. Konno, A. Kobayashi, K. Sakamoto, F. Fagalde, N. E. Katz, H. Saitoh and O. Ishitani, *Inorg. Chim. Acta*, 2000, **299**, 155.
13 (*a*) K. J. Takeuchi, M. S. Thompson, D. W. Pipes and T. J. Meyer, *Inorg. Chem.*, 1984, **23**, 1845; (*b*) F. P. Dwyer, H. A. Goodwin and E. C. Gyarfas, *Aust. J. Chem.*, 1963, **16**, 42.
14 R. C. Young, T. J. Meyer and D. G. Whitten, *J. Am. Chem. Soc.*, 1976, **98**, 286.
15 S. C. Rasmussen, S. E. Ronco, D. A. Mlsna, M. A. Billadeau, W. T. Pennington, J. W. Kolis and J. D. Petersen, *Inorg. Chem.*, 1995, **34**, 821.
16 A. B. Altabef, S. B. R. d. Gallo, M. E. Folquer and N. E. Katz, *Inorg. Chim. Acta*, 1991, **188**, 67.
17 C. R. Hecker, P. E. Fanwick and D. R. McMillin, *Inorg. Chem.*, 1991, **30**, 659.
18 P. T. Gulyas, T. W. Hambley and P. A. Lay, *Aust. J. Chem.*, 1996, **49**, 527.
19 P. A. Adcock, F. R. Keene, R. S. Smythe and M. R. Snow, *Inorg. Chem.*, 1984, **23**, 2336.
20 P. J. Mosher, G. P. A. Yap and R. J. Crutchley, *Inorg. Chem.*, 2001, **40**, 550.
21 E. Sondaz, A. Gourdon, J.-P. Launay and J. Bonvoisin, *Inorg. Chim. Acta*, 2001, **316**, 79.
22 P. J. Mosher, G. P. A. Yap and R. J. Crutchley, *Inorg. Chem.*, 2001, **40**, 1189.
23 E. Sondaz, J. Jaud, J.-P. Launay and J. Bonvoisin, *Eur. J. Inorg. Chem.*, 2002, 1924.
24 D. J. Szalda, F. Fagalde and N. E. Katz, *Acta Crystallogr., Sect. C*, 1996, **52**, 3013.
25 E. C. Constable, M. J. Hannon, A. M. W. C. Thompson, D. A. Tocher and J. V. Walker, *Supramol. Chem.*, 1993, **2**, 243.
26 Based on a CSD search of Version 5.25 (November 2003).
27 W. Haehnel, T. Jansen, K. Gause, R. B. Klösgen, B. Stahl, D. Michl, B. Huvermann, M. Karas and R. G. Herrmann, *EMBO J.*, 1994, **13**, 1028–1038.
28 F. Drepper, M. Hippler, W. Nitschke and W. Haehnel, *Biochemistry*, 1996, **35**, 1282–1295.
29 M. Hippler, J. Reichert, M. Sutter, E. Zak, L. Altschmied, U. Schröer, R. G. Herrmann and W. Haehnel, *EMBO J.*, 1996, **15**, 6374–6384.
30 J. Illerhaus, L. Altschmied, J. Reichert, E. Zak, R. G. Herrmann and W. Haehnel, *J. Biol. Chem.*, 2000, **275**, 17590–17595.
31 B. P. Sullivan, J. M. Calvert and T. J. Meyer, *Inorg. Chem.*, 1980, **19**, 1404.
32 J. M. Calvert, R. H. Schmehl, B. P. Sullivan, J. S. Facci, T. J. Meyer and R. W. Murray, *Inorg. Chem.*, 1983, **22**, 2151.
33 D. C. Ware, P. A. Lay and H. Taube, *Inorg. Synth.*, 1986, **24**, 299.
34 J. Elmsley, *Die Elemente*, W. de Gruyter, Berlin, 1994.
35 *SMART, Data Collection Program for the CCD Area-Detector System; SAINT, Data Reduction and Frame Integration Program for the CCD Area-Detector System*, Bruker Analytical X-ray Systems, Madison, WI, USA, 1997.
36 G. Sheldrick, *Program SADABS: Area-detector absorption correction*, University of Göttingen, Germany, 1996.
37 G. M. Sheldrick, *SHELXS-97, SHELXL-97, Programs for Crystal Structure Analysis*, University of Göttingen, Germany, 1997.
38 (*a*) M. N. Burnett, C. K. Johnson, *ORTEP-III: Oak Ridge Thermal Ellipsoid Plot Program for Crystal Structure Illustrations*, Oak Ridge National Laboratory Report ORNL-6895, 1996; (*b*) L. J. Farrugia, *ORTEP3 for Windows, version 1.076*, University of Glasgow, Scotland, 1997.
39 (*a*) A. L. Spek, *Acta Crystallogr., Sect. A*, 1990, **46**, C34; (*b*) PLATON Version 29-11-98. Windows implementation, L. J. Farrugia, University of Glasgow, Scotland, 1998.
40 A. Gerli, J. Reedijk, M. T. Lakin and A. L. Spek, *Inorg. Chem.*, 1995, **34**, 1836.
41 I. R. Baird, S. J. Rettig, B. R. James and K. A. Skov, *Can. J. Chem.*, 1998, **76**, 1379.

42 FAB-MS of $[Ru(bipy)_2(terpy)](PF_6)_2$ for comparison: X. Liang, S. Suwanrumpha and R. B. Freas, *Inorg. Chem.*, 1991, **30**, 652.
43 M. A. Billadeau, W. T. Pennington and J. D. Petersen, *Acta Crystallogr., Sect. C.*, 1990, **46**, 1105.
44 C.-C. Cheng, J. G. Goll, G. A. Neyhart, T. W. Welch, P. Singh and H. H. Thorp, *J. Am. Chem. Soc.*, 1995, **117**, 2970.
45 H. Nagao, T. Mizukawa and K. Tanaka, *Inorg. Chem.*, 1994, **33**, 3415.
46 R. P. Thummel and Y. Jahng, *Inorg. Chem.*, 1986, **25**, 2527.
47 N. Gupta, N. Grover, G. A. Neyhart, W. Liang, P. Singh and H. H. Thorp, *Angew. Chem., Int. Ed. Engl.*, 1992, **104**, 1058.
48 (*a*) M. Nishio, *CrystEngComm*, 2004, **6**, 130; (*b*) M. Nishio, M. Hirota and Y. Umezawa, *The CH/π interaction (Evidence, Nature and consequences)*, Wiley-VCH, 1998; (*c*) Y. Umezawa, S. Tsuboyama, K. Honda, J. Uzawa and M. Nishio, *Bull. Chem. Soc. Jpn.*, 1998, **71**, 1207; (*d*) C. Janiak, S. Temizdemir, S. Dechert, W. Deck, F. Girgsdies, J. Heinze, M. J. Kolm, T. G. Scharmann and O. M. Zipffel, *Eur. J. Inorg. Chem.*, 2000, 1229.
49 C. Janiak, *J. Chem. Soc., Dalton Trans.*, 2000, 3885.
50 (*a*) π-Interactions between pyridyl-type ligands for comparison: V. Lozan, P.-G. Lassahn, C. Zhang, B. Wu, C. Janiak, G. Rheinwald and H. Lang, *Z. Naturforsch., Teil B*, 2003, **58**, 1152; (*b*) C. Zhang and C. Janiak, *Z. Anorg. Allg. Chem.*, 2001, **627**, 1972; (*c*) C. Zhang and C. Janiak, *J. Chem. Crystallogr.*, 2001, **31**, 29; (*d*) H.-P. Wu, C. Janiak, G. Rheinwald and H. Lang, *J. Chem. Soc., Dalton Trans.*, 1999, 183; (*e*) C. Janiak, L. Uehlin, H.-P. Wu, P. Klüfers, H. Piotrowski and T. G. Scharmann, *J. Chem. Soc., Dalton Trans.*, 1999, 3121; (*f*) H.-P. Wu, C. Janiak, L. Uehlin, P. Klüfers and P. Mayer, *Chem. Commun.*, 1998, 2637.
51 (*a*) N. N. L. Madhavi, A. K. Katz, H. L. Carrell, A. Nangia and G. R. Desiraju, *Chem. Commun.*, 1997, 1953; (*b*) H.-C. Weiss, D. Bläser, R. Boese, B. M. Doughan and M. M. Haley, *Chem. Commun.*, 1997, 1703; (*c*) T. Steiner, M. Tamm, B. Lutz and J. van der Maas, *Chem. Commun.*, 1996, 1127; (*d*) P. L. Anelli, P. R. Ashton, R. Ballardini, V. Balzani, M. Delgado, M. T. Gandolfi, T. T. Goodnow, A. E. Kaifer, D. Philp, M. Pietraszkiewicz, L. Prodi, M. V. Reddington, A. M. Z. Slawin, N. Spencer, J. F. Stoddart, C. Vicent and D. J. Williams, *J. Am. Chem. Soc.*, 1992, **114**, 193.
52 H. Masui, *Coord. Chem. Rev.*, 2001, **219–221**, 957.
53 (*a*) For evidence of metalloaromaticity in aromatic α,α′-diimine–copper(II) chelates, see: E. Craven, C. Zhang, C. Janiak, G. Rheinwald and H. Lang, *Z. Anorg. Allg. Chem.*, 2003, **629**, 2282; (*b*) A. Castiñeiras, A. G. Sicilia-Zafra, J. M. Gonzáles-Pérez, D. Choquesillo-Lazarte and J. Niclós-Gutiérrez, *Inorg. Chem.*, 2002, **41**, 6956.
54 (*a*) DNA binding of Ru complexes: J. A. Smith, J. G. Collins, B. T. Patterson and R. F. Keene, *Dalton Trans.*, 2004, 1277; (*b*) P. U. Maheswari and M. Palaniandavar, *Inorg. Chim. Acta*, 2004, **357**, 901; (*c*) C. Metcalfe and J. A. Thomas, *Chem. Sov. Rev.*, 2003, **32**, 215; (*d*) P. P. Pelligrini and J. R. Aldrich-Wright, *Dalton Trans.*, 2003, 176.
55 K. B. Reddy, M. P. Cho, J. F. Wishart, T. J. Emge and S. S. Isied, *Inorg. Chem.*, 1996, **35**, 7241.
56 G. R. Moore and G. W. Pettigrew, *Cytochromes C: Evolutionary, Structural, and Physicochemical Aspects*, Springer Verlag, Berlin, 1990.
57 R. Apweiler, A. Bairoch, C.-H. Wu, W. C. Barker, B. Boeckmann, S. Ferro, E. Gasteiger, H. Huang, R. Lopez, M. Magrane, M. J. Martin, D. A. Natale, C. O'Donovan, N. Redaschi and L.-S. Yeh, *UniProt: the Universal Protein Knowledgebase Nucleic Acids Res.*, 2004, **32**, D115–D119.
58 G. V. Louie and G. D. Brayer, *J. Mol. Biol.*, 1990, **214**, 527.